Hindawi Publishing Corporation
International Journal of Rotating Machinery
Volume 2016, Article ID 3792645, 14 pages
http://dx.doi.org/10.1155/2016/3792645

Research Article

A New Adaptive Control for Five-Phase Fault-Tolerant Flux-Switching Permanent Magnet Motor

Hongyu Tang,[1] Wenxiang Zhao,[2] and Chenyu Gu[2]

[1]*School of Electrical and Information Engineering, Zhenjiang College, Zhenjiang 212003, China*
[2]*School of Electrical and Information Engineering, Jiangsu University, Zhenjiang 212013, China*

Correspondence should be addressed to Wenxiang Zhao; zwx@ujs.edu.cn

Received 19 September 2016; Accepted 5 December 2016

Academic Editor: Kai Wang

The five-phase fault-tolerant flux-switching permanent magnet (FT-FSPM) motor can offer high efficiency and high fault-tolerant capability. In this paper, its operation principle is presented briefly and its mathematical model is derived. Further, a new adaptive control for an FT-FSPM motor, based on the backstepping method and the sliding mode control strategy, is proposed. According to the backstepping method, the current controllers and voltage control laws are designed to track the speed and minimize the current static error, which enhance the dynamic response and the ability to suppress external disturbances. In order to overcome the influence of parameter variations, according to sliding mode control theory, the virtual control variables and the adaptive algorithm are utilized to approach uncertainty terms. Three Lyapunov functions are designed, and the stability of the closed-loop system is analyzed in detail. Finally, both simulation and experimental results are presented to verify the proposed control method.

1. Introduction

In recent times, flux-switching permanent magnet (PM) (FSPM) motors have gained considerable attention. In the stator, these motors have PMs which are easy to cool, thus reducing the risk of PM demagnetization caused by overheating of the magnets. Moreover, FSPM motors offer a simple rotor structure and good mechanical integrity [1–5]. Hence, they are suitable for high accuracy and high speed operations [6].

In certain high reliability applications, continuous operation of the motor drive is important. The three-phase motors have exhibited a good performance, but they still suffer from limitations under fault conditions [7]. Multiphase PM motors have advantages such as high efficiency, high power density, and phase number redundancy, and they are widely used in special fields such as naval propulsions, aerospace, and military equipment [8]. In the multiphase PM motors, the phase number redundancy ensures that the motor achieves a trouble-free operation and high reliability, even if a phase or a two-phase fault occurs. Recently, by adopting multiphase and fault-tolerant teeth, a five-phase fault-tolerant FSPM (FT-FSPM) motor was proposed, exhibiting merits like high fault tolerance and high reliability.

The precise mathematical model for the FT-FSPM motors is difficult to obtain, because it is a strong nonlinear system with unmeasurable internal and external unknown disturbances [9]. As a result, it is difficult for the linear control schemes to achieve high performance. On the other hand, a variety of advanced intelligent strategies have been introduced to improve the operational performances of the motor drive [10, 11], such as the sliding mode control (SMC) [12], adaptive control [13], fuzzy control [6], neural network control [14], and robust control [15, 16]. Among these control strategies, the SMC has been known to be a very effective way to control the nonlinear system, because it is not sensitive to external disturbances and parameter variations, displays robustness and a fast response, and is easy to implement [17]. However, its sliding mode surface suffers from chattering [18], which affects the control performances. Owing to the uncertainty of parameter variations, low-pass filters and the rotor position compensating methods are

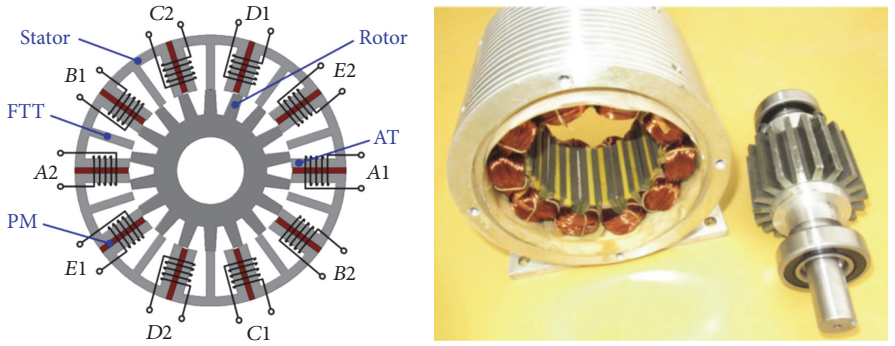

Figure 1: Five-phase FT-FSPM motor. (a) Cross section. (b) Prototype.

used to reduce sliding mode surface chattering [19]. The backstepping control is a control strategy developed recently for uncertain and nonlinear systems, and it can linearize the nonlinear system using the state feedback [15]. The control algorithm can be designed step by step through appropriate Lyapunov functions [20]. The adaptive backstepping observer and the backstepping integral were presented to improve the robustness and tracking accuracy, but there still exist static errors and larger speed overshoots [21–23]. The combination of the backstepping control and the SMC has become a major strategy in the field of study of uncertain nonlinear systems. So far, the backstepping SMC method for the FT-FSPM motor system has almost never been reported.

This paper proposes a new backstepping SMC method for the FT-FSPM motors, which can remarkably suppress sliding mode chattering and accurately track the motor speed. Intermediate virtual control variables and the $d-q$ axis voltage control laws are designed to achieve the desired motor speed and position control, ensuring the stability of the system. The external interferences and internal mechanical parameter variations are collectively referred to as the uncertainty terms, which are approached by the adaptive learning algorithm, access to the best state of the system.

2. FT-FSPM Motor

Figure 1 shows the cross section of a five-phase FT-FSPM motor. This motor has 10 stator slots and 18 rotor poles. Its rotor is similar to that of a switched reluctance motor [24]. The curial merit of this topology is the introduction of fault-tolerant teeth, which interleave with the armature teeth. In contrast, the stator of a conventional FSPM motor consists of many U-shaped laminated segments. The five-phase FT-FSPM motor consists of 10 "E"-shaped units, namely, E-cores, and a concentrated armature coil is wound around every two units, while a piece of magnet is embedded in the middle of two E-cores. Thus, the phase windings of adjacent stator poles are essentially isolated, leading to the merits of phase decoupling. Therefore, this motor has good fault-tolerant capability, which can ensure high reliability of the motor system. Besides, owing to the additional teeth, it has less mutual inductance [25].

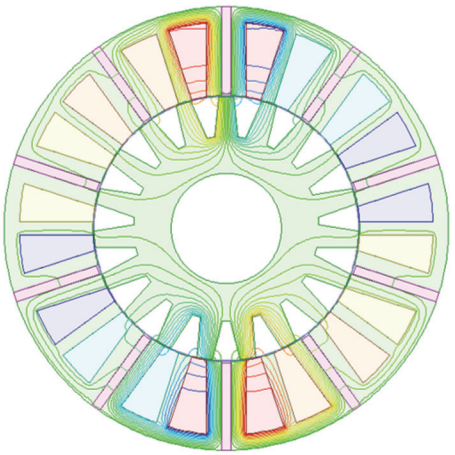

Figure 2: Magnetic field distributions of FT-FSPM motor by armature current only.

As shown in Figure 2, according to the principle of minimum reluctance, the flux will flow down from the stator core yoke as much as possible. Therefore, the armature reaction has no impact on PMs.

3. Mathematical Model

Although the FT-FSPM motor has PMs in the stator, its PM flux and back EMF (Electromotive Force) appear bipolar sinusoidal under no load. Hence, its fundamental coordinate system can be described as shown in Figure 3.

The simplified mathematical model of the FT-FSPM motor can be obtained by the coordinate transformation, and the motor system can be reduced, decoupled, and linearized. Since the motor has ideal sinusoidal flux linkage, only the fundamental flux linkage is considered in this work. According to the law of the magnetic circuit, the magnet equation is described as

$$\begin{aligned} \psi_d &= \left(L_s + 2.5L_{md1}\right) i_d + \psi_m, \\ \psi_q &= \left(L_s + 2.5L_{mq1}\right) i_q, \end{aligned} \tag{1}$$

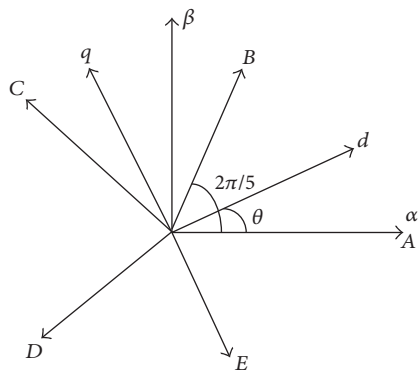

Figure 3: Five-phase fundamental coordinates of the FT-FSPM motor.

where L_s is the leakage inductance, i_d and i_q are currents along the d and q axes respectively, ψ_m is the PM flux, L_{md1} and L_{mq1} are the stator inductances along the d and q axes, respectively, and ψ_d and ψ_q are the flux along the d and q axes, respectively. By the 5/2 coordinate transformation, the currents along the d and q axes, that is, i_d and i_q, are expressed as

$$\begin{aligned} i_d &= \frac{2}{3}\left[\cos\theta i_A + \cos\left(\theta - \frac{2}{5}\pi\right) i_B + \cos\left(\theta - \frac{4}{5}\pi\right) i_C \right. \\ &\quad \left. + \cos\left(\theta + \frac{4}{5}\pi\right) i_D + \cos\left(\theta + \frac{2}{5}\pi\right) i_E\right], \\ i_q &= \frac{2}{3}\left[-\sin\theta i_A - \sin\left(\theta - \frac{2}{5}\pi\right) i_B - \sin\left(\theta - \frac{4}{5}\pi\right) i_C \right. \\ &\quad \left. - \sin\left(\theta + \frac{4}{5}\pi\right) i_D - \sin\left(\theta + \frac{2}{5}\pi\right) i_E\right], \end{aligned} \tag{2}$$

where i_A, i_B, i_C, i_D, and i_E are the five-phase currents and θ is the position angle of the rotor. From (2), the five-phase currents are transferred to the two-phase currents of the rotating coordinate system. Owing to the adoption of the field orient control, it is necessary to know the relationship between the currents, voltages, and torque in the rotating coordinate system. The stator voltage and electromagnetic torque equations of the rotor coordinate system can be described as

$$\begin{aligned} u_d &= r_s i_d - \omega\left(L_s + \frac{5}{2}L_{mq1}\right) i_q + \left(L_s + \frac{5}{2}L_{md1}\right)\frac{di_d}{dt}, \\ u_q &= r_s i_q + \omega\left(L_s + \frac{5}{2}L_{md1}\right) i_d + \omega\psi_m \\ &\quad + \left(L_s + \frac{5}{2}L_{mq1}\right)\frac{di_q}{dt}, \\ T_e &= 2.5 n_p\left[\psi_m i_q + \left(L_{md1} - L_{mq1}\right) i_d i_q\right], \end{aligned} \tag{3}$$

where n_p is the pairs number of rotor pole, u_d and u_q are the voltages along the d and q axes respectively, ω is the rotor angular speed, r_s is the stator resistance, and T_e is the electromagnetic torque. Although the d-axis inductance is not equal to the q-axis inductance, the difference between them is little. As evident from (3), the electromagnetic torque of the FT-FSPM motor is mainly related to the d-q axis current and inductance. According to Newton's laws of motion, without considering the elastic torsional moment coefficient and the motor mechanical movement, the motion equation is expressed as

$$\begin{aligned} T_e &= J\frac{d\omega}{dt} + B\omega + T_l, \\ \omega &= \frac{d\theta}{dt}, \end{aligned} \tag{4}$$

where J is the moment of inertia, B is the viscous friction coefficient, and T_l is the load torque.

4. Controller Design

4.1. Design of Backstepping Control. It is clear that the model of a FT-FSPM motor has a high nonlinear characteristic, because there exists a coupling between the currents i_d and i_q, and the rotor angular speed ω. The block diagram of the FT-FSPM motor drive system based on the backstepping SMC is shown in Figure 4. The FT-FSPM motor drive adopts $i_d = 0$ control strategy on field orientation. According to the space vector control principle, the five-phase motor stator currents generate α-β axis currents according to the 5/2 transformation. Subsequently, the d-q axis currents are generated by the Park transformation and they are sent into the controller. Since the electromagnetic torque T_e is linearly proportional to the q-axis current i_q, the torque output can be controlled by adjusting the current i_q. The backstepping controller realizes the current closed-loop control and generates control voltages u_d and u_q in the FT-FSPM motor drive system. Subsequently, the space vector pulse width modulation (PWM) is generated by the 2/5 coordinate transformation. The adaptive sliding mode controller is use to identify external interferences and internal parameter variations. Load torque estimation is used to estimate T_l according to the adaptive law.

In practice, the load torque of the FT-FSPM motor usually changes and the parameter uncertainties can deteriorate the operational performance. The traditional proportional integral derivative control cannot provide a satisfactory performance because the parameters are fixed. Therefore, the speed identification system usually suffers from disturbances. When the motor operates, its internal parameters and external interferences may have fluctuations. Accordingly, the backstepping controller is used to improve the anti-interference ability and the adaptive sliding mode algorithm is adopted to estimate the uncertainty terms.

In case of the existing SMC, the chattering problem is inevitable during the process of the sliding mode switching and it affects the stability of the system. To reduce or eliminate sliding mode chattering, the backstepping control strategy is applied to the SMC algorithm. A new backstepping SMC

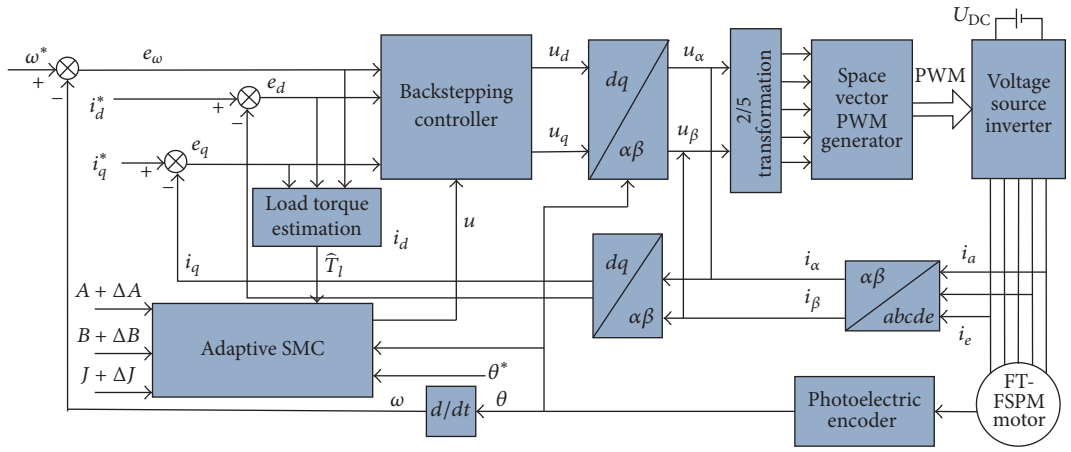

Figure 4: Block diagram of the FT-FSPM motor system.

method replaces traditional proportional integral derivative control. Compared to the existing SMC method, the backstepping SMC is not sensitive to internal parameter variations and external interferences, which can ensure that the system trajectory reaches and stays on the sliding mode surface. The adaptive sliding mode controller can automatically track parameter changes and adjust the control variable u.

The design of backstepping control for the FT-FSPM motor system consists of two steps. First, the speed subsystem is designed using the voltage control law, which guarantees speed stability. Subsequently, for the current subsystem, a robust control law is designed to realize the current track. It is assumed that ω^* is the desired speed signal and ω is the actual speed signal. They are enough smooth. The speed tracking error signal is defined as

$$e_\omega = \omega^* - \omega. \tag{5}$$

The derivation of e_ω is given by

$$\dot{e}_\omega = \dot{\omega}^* - \dot{\omega} = \dot{\omega}^* + \frac{1}{J}\left[T_l + B\omega - \frac{5}{2}n_p\psi_m i_q - \frac{5}{2}n_p\left(L_{md1} - L_{mq1}\right)i_d i_q\right]. \tag{6}$$

For the speed subsystem, the first Lyapunov function is defined as $V_1 = (1/2)e_\omega^2$, and its derivation is expressed as

$$\dot{V}_1 = e_\omega\dot{e}_\omega = \frac{e_\omega}{J}\left[J\dot{\omega}^* + T_l + B\omega - \frac{5}{2}n_p\psi_m i_q - \frac{5}{2}n_p\left(L_{md1} - L_{mq1}\right)i_d i_q\right] = -ke_\omega^2 + \frac{e_\omega}{J}\left[J\dot{\omega}^* + T_l + B\omega - \frac{5}{2}n_p\psi_m i_q - \frac{5}{2}n_p\left(L_{md1} - L_{mq1}\right)i_d i_q + kJe_\omega\right], \tag{7}$$

where k is the speed feedback gain and it is a positive constant. In (7), apart from the speed term, there are current terms and the speed error term. Therefore, the desired values of the current control terms i_d^* and i_q^* are defined as

$$i_d^* = 0,$$
$$i_q^* = \frac{2}{5n_p\psi_m}\left(J\dot{\omega}^* + T_l + B\omega + kJe_\omega\right). \tag{8}$$

Accordingly, the currents i_d and i_q will converge to i_d^* and i_q^*, so that $i_d = i_d^*$ and $i_q = i_q^*$. Therefore, (8) can be substituted into (7). Subsequently, (7) becomes $\dot{V}_1 = -ke_\omega^2 < 0$, which satisfies the speed convergence requirements. However, the load torque T_l is unknown in the actual operation and it is replaced by the estimated value of load torque $\widehat{T}_l$. According to the vector control theory, the current i_d is always forced to be zero, in order to orient all the linkage flux in the d-axis. Therefore, the d-q axis current tracking errors are defined as

$$e_d = i_d^* - i_d,$$
$$e_q = i_q^* - i_q. \tag{9}$$

When (8) and (9) are substituted into (6), the form is expressed as

$$\dot{e}_\omega = \frac{1}{J}\left[\frac{5}{2}n_p\psi_m e_q + \frac{5}{2}n_p\left(L_{md1} - L_{mq1}\right)e_d i_q - \widetilde{T}_l - kJe_\omega\right], \tag{10}$$

where $\widetilde{T}_l$ is estimation error, $\widetilde{T}_l = \widehat{T}_l - T_l$.

The core of the motor driving system is made of the five-phase currents from the inverter output and they are controlled by the space vector PWM. The current loop is a closed-loop. Therefore, the current control of i_d and i_q is the key for the FT-FSPM motor. According to the sliding mode

theory, the derivative form of the current error is described as

$$\begin{aligned}\dot{e}_d &= \frac{R_s i_d - n_p \omega L_{mq1} i_q - u_d}{L_{md1}},\\ \dot{e}_q &= \frac{2(B-KJ)}{5n_p\psi_m J}\left\{\frac{5n_p}{2}\left[\psi_m i_q + \left(L_{md1}-L_{mq1}\right) i_d i_q\right]\right.\\ &\quad \left. - B\omega - \widehat{T}_l\right\} + \frac{R_s i_q + n_p\omega L_{md1} i_d + n_p\omega\psi_m - u_q}{L_{mq1}}\\ &\quad + \frac{2}{5n_p\psi_m}\left(J\ddot{\omega}^* + \dot{\widehat{T}}_l + KJ\dot{\omega}^*\right).\end{aligned} \tag{11}$$

Furthermore, in order to eliminate the derivative term of the q-axis current error in the control algorithm, the second Lyapunov function is defined as

$$V_2 = V_1 + \frac{1}{2}e_d^2 + \frac{1}{2}e_q^2 + \frac{1}{2\lambda}\widetilde{T}_l^2. \tag{12}$$

Further,

$$\begin{aligned}\dot{V}_2 &= e_\omega \dot{e}_\omega + e_d\dot{e}_d + e_q\dot{e}_q + \frac{\widetilde{T}_l\dot{\widehat{T}}_l}{\lambda}\\ &= -ke_\omega^2 - k_d e_d^2 - k_q e_q^2 + e_\omega\left(\dot{e}_\omega + ke_\omega\right)\\ &\quad + e_d\left(\dot{e}_d + k_d e_d\right) + e_q\left(\dot{e}_q + k_q e_q\right) + \frac{\widetilde{T}_l\dot{\widehat{T}}_l}{\lambda}.\end{aligned} \tag{13}$$

To guarantee the global asymptotic stability in the current loop, the d-q axis control voltages are designed as

$$\begin{aligned}u_d &= R_s i_d - n_p\omega L_{mq1} i_q + k_d L_{md1} e_d,\\ u_q &= R_s i_q + n_p\omega L_{md1} i_d + n_p\omega\psi_m + k_q L_{mq1} e_q\\ &\quad - \frac{2L_{mq1}}{5n_p\psi_m J}(B-kJ)\left[\frac{5n_p\psi_m}{2}e_q\right.\\ &\quad \left. + \frac{5n_p}{2}\left(L_{md1}-L_{mq1}\right)e_d i_q + B\omega + \widehat{T}_l\right]\\ &\quad - \frac{2}{5n_p\psi_m}\left(J\ddot{\omega}^* + \dot{\widehat{T}}_l + kJ\dot{\omega}^*\right).\end{aligned} \tag{14}$$

The load torque estimation law is described as

$$\dot{\widehat{T}}_l = \lambda\left[\frac{e_\omega}{J} - \frac{2(B-kJ)}{5n_p\psi_m J}e_q\right]. \tag{15}$$

Further, (14) and (15) are substituted into (13), and the form is expressed as

$$\dot{V}_2 = -ke_\omega^2 - k_d e_d^2 - k_q e_q^2, \tag{16}$$

where k_d and k_q are positive constants. Subsequently, (16) becomes $\dot{V}_2 \leq 0$. It satisfies the asymptotically stable condition of the system. For the FT-FSPM motor drive system, the tracking errors e_ω, e_d, and e_q converge toward zero. The voltage control law is a concrete way to achieve the backstepping strategy for the motor system.

4.2. Adaptive Sliding Mode Controller Design. Notably, the controller design does not consider changes from the parameters of the motor itself. In the actual operation, the parameters r_s, B, J, and T_l can change with the speed variation and the external interferences. These factors will affect the stability of the FT-FSPM motor drive system and lower the system control accuracy. Although the upper bound of the uncertainty term is difficult to determine, effective estimations of the uncertainty term can be achieved using the adaptive sliding mode algorithm. The motion equation is rewritten as

$$\begin{aligned}\dot{\omega} &= \frac{1}{J}\left[\frac{5}{2}n_p\psi_m i_q + \frac{5}{2}n_p\left(L_{md1}-L_{mq1}\right)i_d i_q - T_l\right.\\ &\quad \left. - B\omega\right].\end{aligned} \tag{17}$$

It is simplified as follows:

$$\dot{\omega} = Au - \frac{B}{J}\omega - \frac{T_l}{J}, \tag{18}$$

where $A = (1/J)[(5/2)n_p\psi_m i_q + (5/2)n_p(L_{md1} - L_{mq1})i_d]$. Because the current i_q is the key to motor control, the control term is selected as $u = i_q$. The estimated value of the load torque $\widehat{T}_l$ replaces T_l. In order to improve the control accuracy and performance of the FT-FSPM motor, the changes in the uncertainty terms are considered, and

$$\dot{\omega} = (A+\Delta A)u - \frac{(B+\Delta B)}{J+\Delta J}\omega - \frac{\left(\widehat{T}_l + \Delta\widehat{T}_l\right)}{J+\Delta J}, \tag{19}$$

where ΔA contains the variations caused by the changing resistance r_s

$$\dot{\omega} = Au + B_m\omega + F, \tag{20}$$

where F is regarded as the total uncertainty term; that is, $F = \Delta Au - (\Delta B/(J+\Delta J))\omega - (\widehat{T}_l + \Delta\widehat{T}_l)/(J+\Delta J)$, and $B_m = -B/(J+\Delta J)$. Further, $\Delta A, \Delta B$, and $(\widehat{T}_l + \Delta\widehat{T}_l)/(J+\Delta J)$ are uncertainty terms of the motor parameter variations and external load interferences. In order to facilitate analysis, the rotor position angle of the motor is introduced to analyze the uncertainty terms. Further, x_1 is defined as the rotor position angle error; that is, $x_1 = \theta - \theta^*$, and the derivative form is $\dot{x}_1 = \omega - \dot{\theta}^*$. Further, x_2 is a virtual control term. Subsequently, the position angle speed ω can be expressed using x_1 and x_2 as follows:

$$\omega = x_2 + \dot{\theta}^* - c_1 x_1, \tag{21}$$

where $x_2 = \omega - \dot{\theta}^* + c_1 x_1$ and thus $\dot{x}_1 = \omega - \dot{\theta}^* = x_2 - c_1 x_1$.

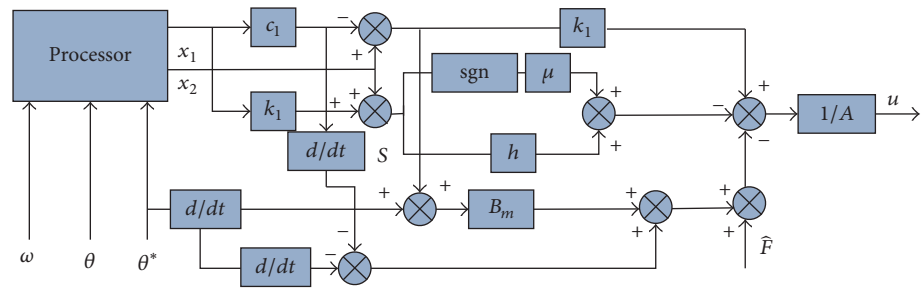

Figure 5: Block of the adaptive sliding mode controller.

To overcome the interferences and parameter variations, the sliding mode term is introduced. The selection of sliding mode switching function is very important. For easy operation and less sliding mode chattering, taking into account the prior backstepping control analysis, the sliding mode surface is selected as

$$S = kx_1 + x_2. \tag{22}$$

The derivative form is expressed as

$$\dot{S} = k\dot{x}_1 + \dot{x}_2. \tag{23}$$

To verify the feasibility of above assumptions, the third Lyapunov function is defined as

$$V_3 = V_2 + \frac{1}{2}x_1^2 + \frac{1}{2}S^2 + \frac{1}{2\gamma}\widetilde{F}^2. \tag{24}$$

The derivative form of (24) is given by

$$\begin{aligned}\dot{V}_3 &= \dot{V}_2 + \frac{1}{2}x_1^2 + \frac{1}{2}S^2 + \frac{1}{2\gamma}\widetilde{F}^2 = \dot{V}_2 + x_1x_2 - cx_1^2 \\ &+ S\dot{S} - \frac{1}{\gamma}\widetilde{F}\dot{\widehat{F}} = \dot{V}_2 + x_1x_2 - cx_1^2 \\ &+ S\left(k_1\left(x_2 - c_1x_1\right) + B_m\left(x_2 + \dot{\theta}^* - c_1x_1\right) + Au\right. \\ &\left.+ F - \ddot{\theta}^* + c_1\dot{x}_1\right) - \frac{1}{\gamma}\widetilde{F}\dot{\widehat{F}} = \dot{V}_2 + x_1x_2 - cx_1^2 \\ &+ S\left(k_1\left(x_2 - c_1x_1\right) + B_m\left(x_2 + \dot{\theta}^* - c_1x_1\right) + Au\right. \\ &\left.+ \widehat{F} - \ddot{\theta}^* + c_1\dot{x}_1\right) - \frac{1}{\gamma}\widetilde{F}\left(\dot{\widehat{F}} + \gamma S\right),\end{aligned} \tag{25}$$

where γ is positive constant and $\widehat{F}$ is the estimated value of F. Further, $\widetilde{F}$ is the estimation error and $\widetilde{F} = F - \widehat{F}$. Assuming that the parameter variations and external interferences are slow, the uncertainty term can be approximated as a constant where $|F| \le F_m$, and F_m is the max of F. In this paper, the exponential approaching law is adopted and the form is $-hS - u\,\mathrm{sgn}(S)$. The exponential term $-hS$ can guarantee a greater speed to approach the sliding surface away from the switching surface. However, a simple exponential term cannot guarantee limited arriving time and the constant speed term $u\,\mathrm{sgn}(S)$ is added. When S is close to zero and the approaching speed is u instead of zero, it ensures limited arriving time. Therefore, the adaptive controller is designed as

$$\begin{aligned}u = A^{-1}\left[-k_1\left(x_2 - c_1x_1\right) - B_m\left(x_2 + \dot{\theta}^* - c_1x_1\right) - \widehat{F}\right. \\ \left.+ \ddot{\theta}^* - c_1\dot{x}_1 - hS - \mu\,\mathrm{sgn}\left(S\right)\right].\end{aligned} \tag{26}$$

The adaptive law is designed as

$$\dot{\widehat{F}} = -\gamma S. \tag{27}$$

Subsequently, (26) and (27) are substituted into (25), resulting in the following:

$$\begin{aligned}\dot{V}_3 &= -ke_\omega^2 - k_de_d^2 - k_qe_q^2 + x_1x_2 - c_1x_1^2 - hS^2 \\ &- \mu\left|S\right|,\end{aligned} \tag{28}$$

$Q = \begin{bmatrix} c_1 + hk_1^2 & hk_1 - 1/2 \\ hk_1 - 1/2 & h \end{bmatrix}$, and $X^T = \begin{bmatrix} x_1 & x_2 \end{bmatrix}$. These equations are substituted into (28); then

$$\dot{V}_3 = -ke_\omega^2 - k_de_d^2 - k_qe_q^2 - X^TQX - \mu\left|S\right| \le 0. \tag{29}$$

Taking into account the values of h, c_1, and k_1, Q is guaranteed to be a positive definite matrix. Subsequently, (29) becomes $\dot{V}_3 \le 0$. According to the Lyapunov stability theory, the FT-FSPM motor system is stable. The block of the adaptive sliding mode controller is shown in Figure 5. The rotor angle speed signal ω, the position angle signal θ, and θ^* are the inputs of the controller. In this regard, the purpose of increasing the virtual control terms is to design the adaptive sliding mode algorithms to approach the total uncertainty term.

5. Simulation and Experimental Results

5.1. Simulation Results. To verify the effectiveness of the backstepping SMC algorithm, a simulation model is built using MATLAB/Simulink. The five-phase FT-FSPM motor parameters are as follows: the rated power $P = 1.8$ kW, the phase voltage $U = 200$ V, the rated speed $n = 600$ r/min, the

rated torque $T_e = 7.8$ N·m, the stator resistance $r_s = 2.56\ \Omega$, the winding inductances $L_{md1} = 36$ mH and $L_{mq1} = 35$ mH, the moment of inertia $J = 0.00062$ kg·m^2, the friction coefficient $B = 0.00031$ N·m·s, and the permanent magnet flux $\psi_m = 0.183$ Wb.

The parameters of the backstepping SMC are selected as

$$\begin{aligned} \eta &= 0.3, \\ \beta &= 1.5, \\ \gamma &= 12, \\ \mu &= 0.1, \\ k_1 &= 15, \\ c_1 &= 10, \\ h &= 20. \end{aligned} \tag{30}$$

To test the robustness of the controller against changes in the load, the simulations are performed under two different cases. The reference speed is $\omega^* = 600$ r/min. In the first case, at $t = 0.2$ s, the load torque T_l is changed from 5 N·m to 7.5 N·m, and the result is shown in Figure 6. In the other case, at $t = 0.3$ s, the load torque T_l is changed from 5 N·m to 2.5 N·m.

As seen from Figures 6 and 7, at the start, the simulation results of the proposed SMC show that the speed response can quickly track the reference speed within 0.01 s, but the existing SMC lags by 0.05 s. Notably, the speed overshoot in the case of the proposed SMC can be reduced from 10% to 7.5%, compared to the existing SMC. Moreover, the existing SMC causes the currents i_d and i_q to produce large chattering initially, but the proposed SMC can minimize instant chattering due to the effectiveness of the voltage (u_d, u_q) control laws and the sliding mode control algorithm. It can be seen that the d-axis current i_d is well decoupled from the motor speed and is regulated to zero. T_e is proportional to the q-axis current and is almost simultaneous to the changing current i_q. When the motor starts, because of the FT-FSPM motor location torque, there are large electromagnetic torque and current spikes. However, the electromagnetic torque ripple is small under normal operation. The response trajectories of the five-phase currents are consistent with the results of the theoretical analysis and tend to steady within 0.01 s. They present sine waves and corresponding changes in the amplitude. In the instant of the load torque mutations, the speed, current, and torque fluctuations of the proposed SMC are smaller than those of the existing SMC, although the response rapidity is almost same. Therefore, the proposed SMC method promises better implementation as compared to the existing SMC method for the FT-FSPM motor system.

In order to test the speed tracking performance of the FT-FSPM motor under changing speed, within 0.25 s, the speed is increased from 600 r/min to 800 r/min and the speed is decreased from 600 r/min to 400 r/min, respectively. As shown in Figures 8 and 9, by using the proposed SMC algorithm, the response speed can quickly track the reference speed signal and the speed tracking error is very small. As can be seen from the simulation of the rotor position angle, the response of the rotor position angle can reflect the changes in speed.

With regard to the uncertainty terms, the simulations of the rotor position angle are designed to validate the feasibility of the algorithm and the performance of the position tracking. A sinusoidal signal is taken as the input signal. Figure 10 shows the tracking of the motor position angle and the trajectories of the controller input when a load of 0.2 N·m is applied to the system at the rotor position angle $\theta = 90^\circ$. Figure 11 shows the tracking of the motor position angle and the trajectories of the controller input when the interference is applied to the system at the rotor position angle $\theta = 270^\circ$. In spite of the abrupt application of load, the rotor can track the ideal position after a transient fluctuation. Although mutation changes caused by the uncertainty terms are present, the time taken for adjustment of the position angle is very short and the fluctuation is small. The control input has a very quick response and the total uncertainty term is supposed to be a sinusoidal signal. Figure 12 shows that $\widehat{F}$ can track F adaptively and realize the estimation of uncertainty terms using the adaptive sliding mode algorithm.

5.2. Experimental Results. To verify the feasibility of the proposed SMC further, an experimental platform for the FT-FSPM motor control was built in the laboratory, as shown in Figure 13. The experimental platform devices include a DSP2812 chip, a Mitsubishi IPM, a 2048 line photoelectric encoder, a power module, Hall sensors, a torque sensor, and power and driver modules. A DC motor is used as the load. The experimental results are shown as follows.

The experimental results under a speed of 200 r/min are shown in Figures 14 and 15. Figure 14 shows that the currents have a big transient fluctuation when the load increases from 4 N·m to 6 N·m. It can be observed that the torque and the speed fluctuations of the proposed SMC are substantially smaller than those of the existing SMC. The speed response of the proposed SMC is approximately 0.3 s faster than that of the existing SMC. After changing the load, the current changed significantly. Figure 15 shows that the current and torque ripples have been reduced significantly under the proposed SMC method, when the load decreases from 6 N·m to 4 N·m. The speed response of the proposed SMC is approximately 0.4 s faster than that of the existing SMC. After 1–1.5 s, the speed, the currents, and the torque tend to be steady. Obviously, the fluctuation of the proposed SMC method is significantly smaller, indicating that the proposed SMC can absorb the sudden load changes better and has an anti-interference capability. Compared to the existing SMC, the proposed SMC can improve the robustness and the rapidity of the FT-FSPM motor drive system.

The experimental waveforms of currents i_d and i_q are shown in Figure 16. Accordingly, because of the adopted $i_d = 0$ control strategy, the current i_d is almost a straight line at zero, while the current i_q also changes with the changing

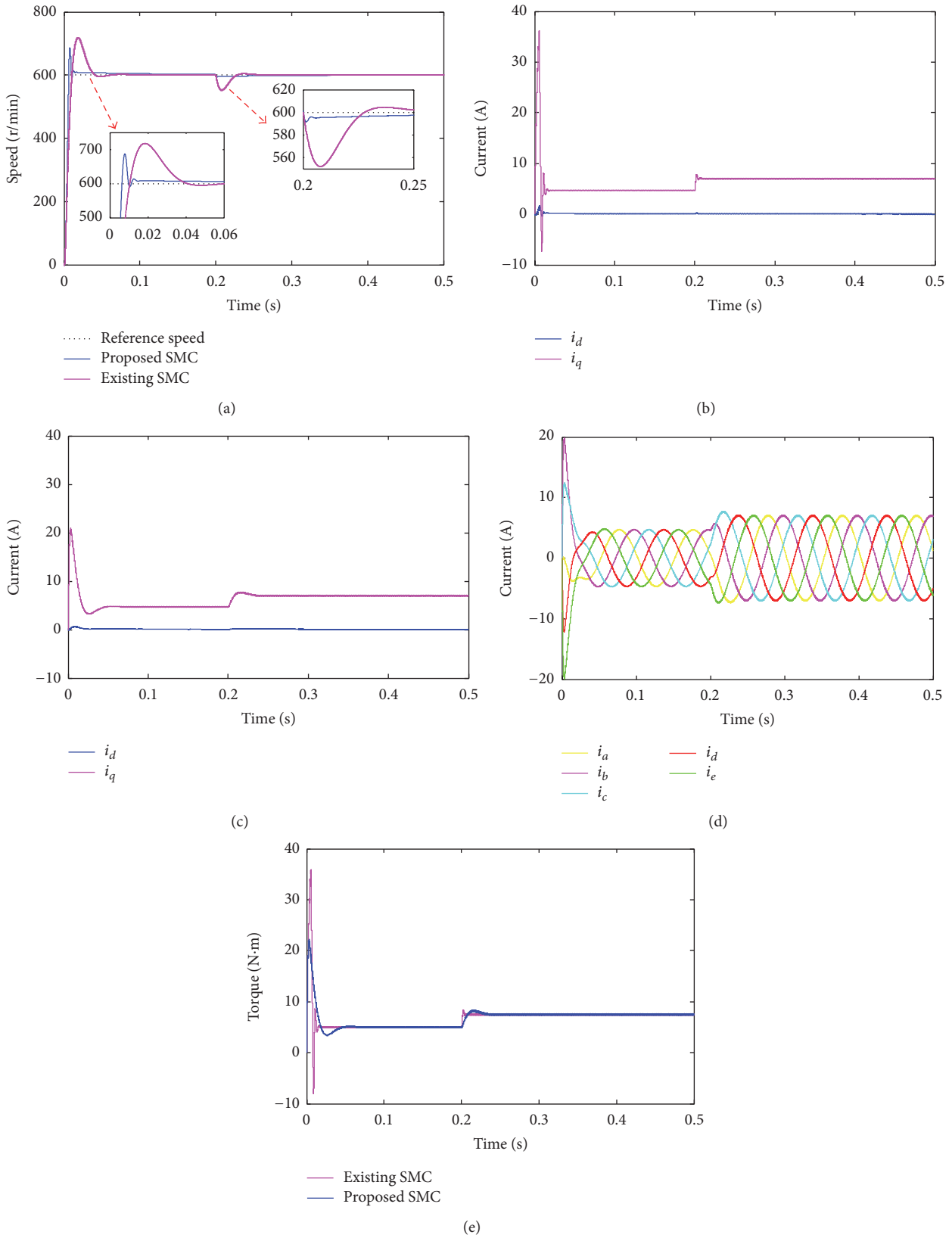

FIGURE 6: Simulation results when increasing load from 5 N·m to 7.5 N·m. (a) Speed response. (b) Current waveforms i_d and i_q under the existing SMC. (c) Current waveforms i_d and i_q under the proposed SMC. (d) Waveforms of the five-phase currents. (e) Torque response.

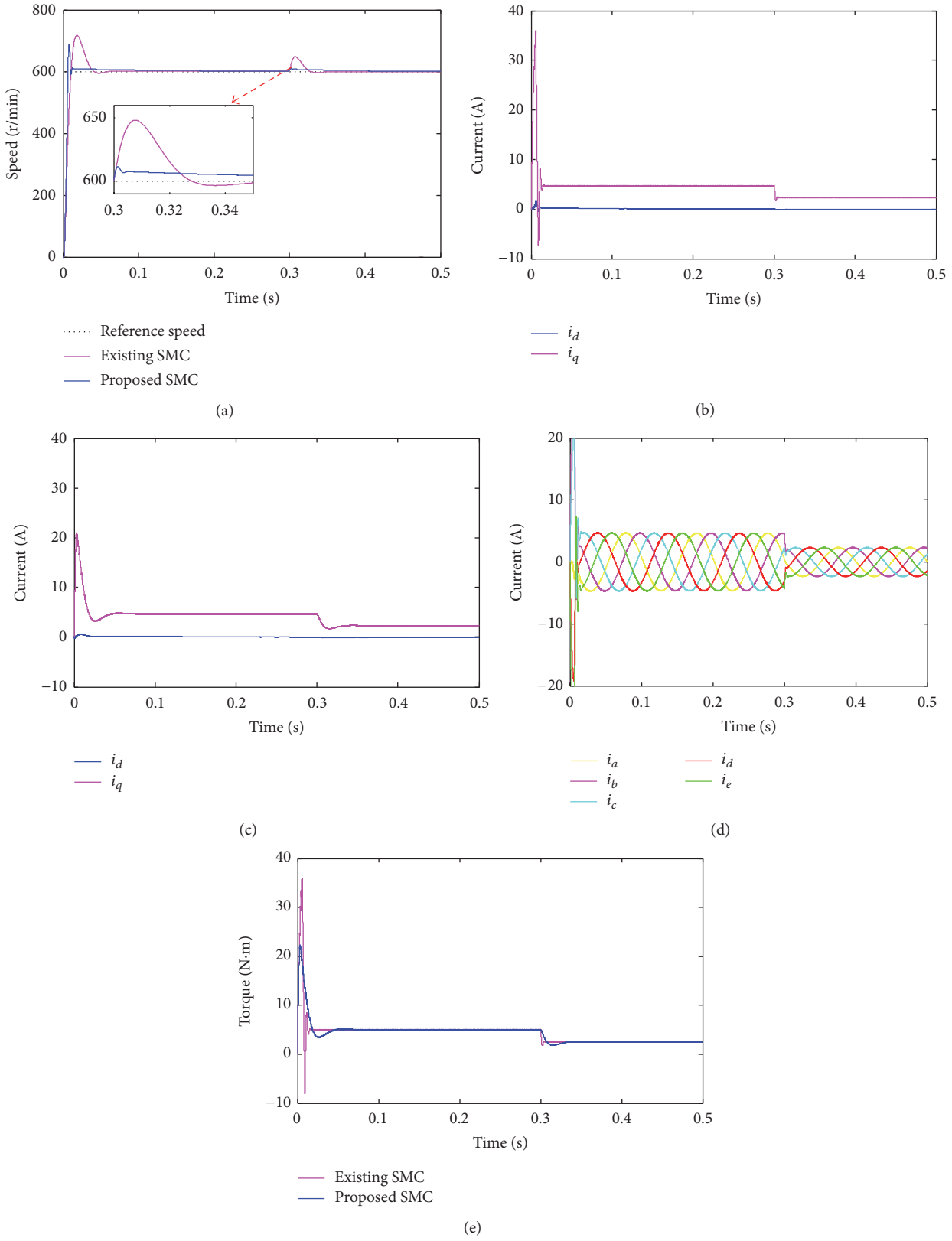

FIGURE 7: Simulation results when decreasing load from 5 N·m to 2.5 N·m. (a) Speed response. (b) Current waveforms i_d and i_q under the existing SMC. (c) Current waveforms i_d and i_q under the proposed SMC. (d) Waveforms of the five-phase currents. (e) Torque response.

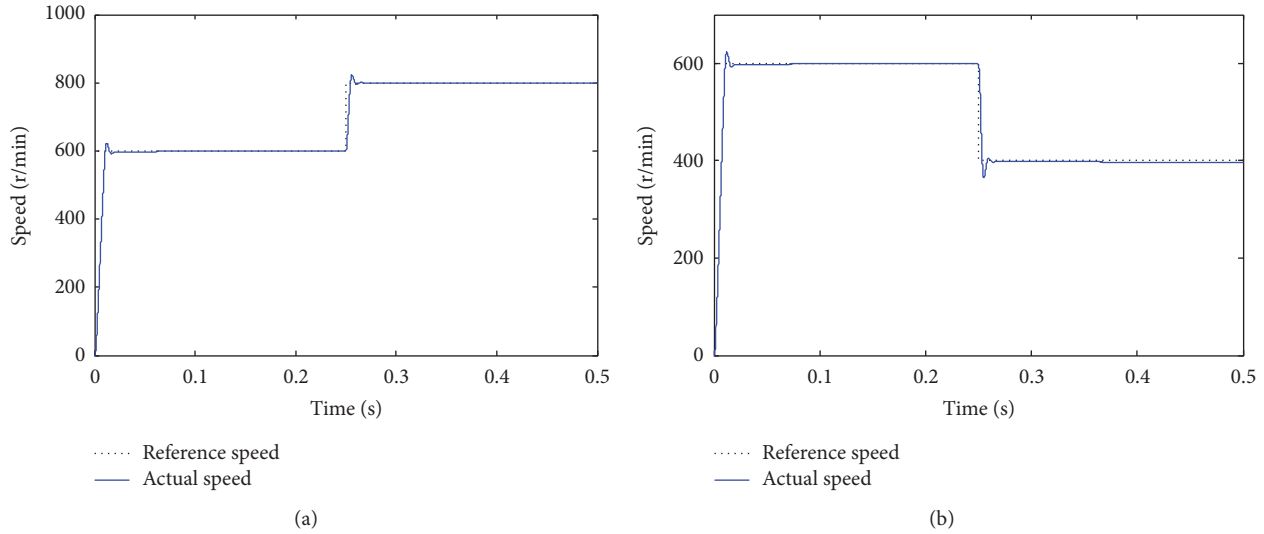

Figure 8: Speed tracking under speed changing. (a) Speed increasing. (b) Speed decreasing.

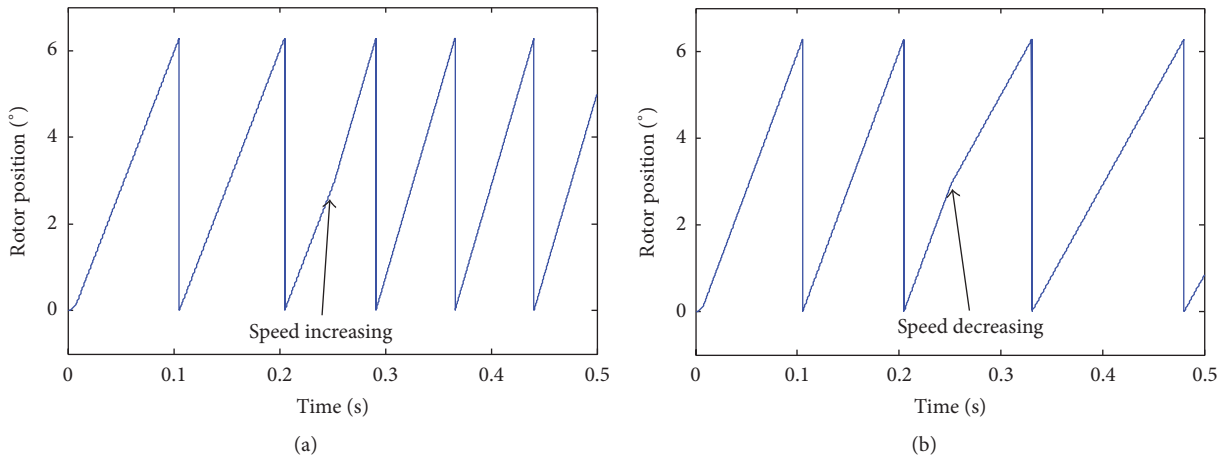

Figure 9: Rotor position angle tracking under changing speed. (a) Speed increasing. (b) Speed decreasing.

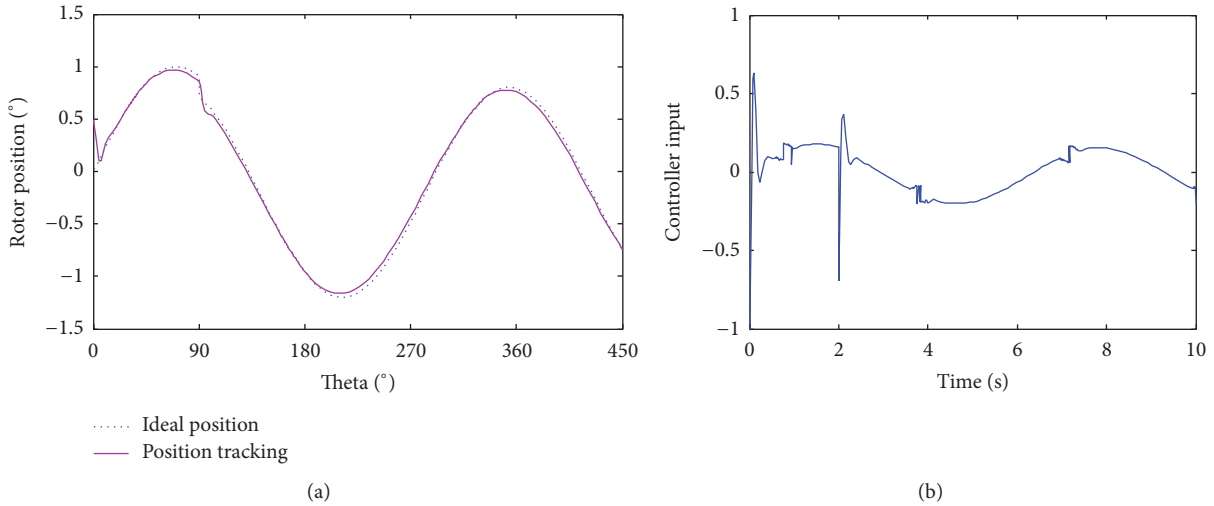

Figure 10: Simulation results of the backstepping SMC when the load is applied. (a) Position tracking. (b) Control input.

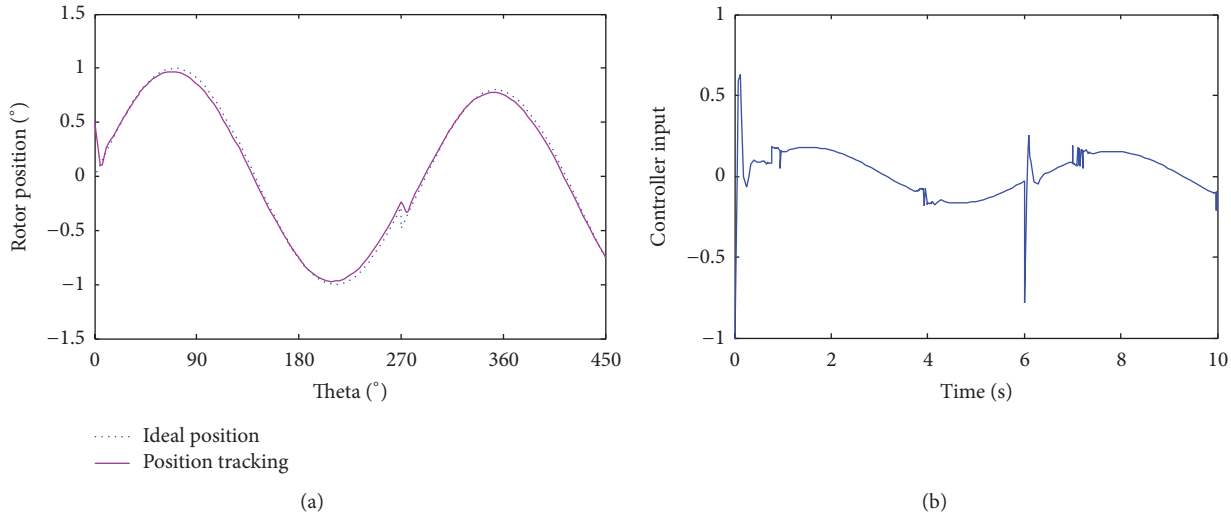

Figure 11: Simulation results of the backstepping SMC when the interference is applied. (a) Position tracking. (b) Control input.

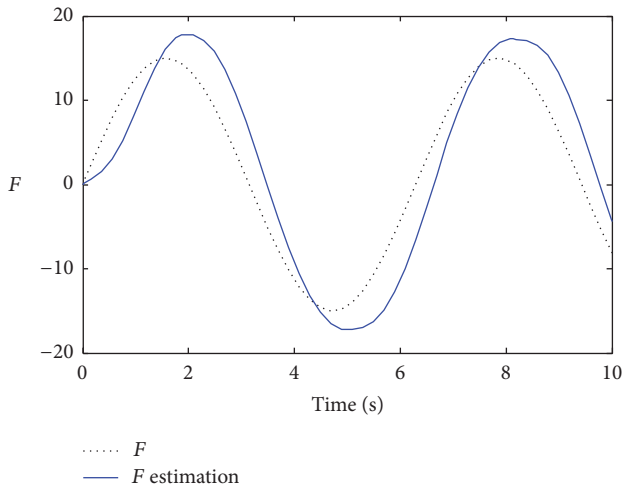

Figure 12: Adaptive tracking trajectory of F.

load. Owing to the proposed SMC method, the rapidity of response of current i_q is improved and the speed response time decreases by approximately 0.1 s. At the instant the load changes, there exist small fluctuations and almost no overshoot. When the motor operates normally, the current ripple is also significantly reduced, by approximately 10 to 15%. These results indicate that this method is superior to the existing SMC, in terms of both the rapidity and the robustness.

6. Conclusion

The five-phase FT-FSPM motor has a simple rotor structure and high fault-tolerant capability, which is effective to the PM fever and faulty problems. To reduce the influences of the system parameter uncertainties and external interferences, a nonlinear adaptive SMC algorithm has been proposed for the FT-FSPM motor, based on the backstepping control theory. The introduction of the virtual control terms, the speed tracking error, and the estimated errors of the d-q axis currents are the control terms, and the voltage control laws are designed using the backstepping method. These can improve the system robustness, and the dynamic and static performances under time-varying load torques, owing to the adaptive SMC algorithm for the uncertainty terms. The proposed SMC can effectively achieve speed tracking and reduce the chattering, and the system stability under this method has been demonstrated. It ensures that the five-phase FT-FSPM motor has better transient performance and the stability of the motor system has been secured. The simulations and the experimental results confirm the validity of the proposed method. In view of the characteristics of the

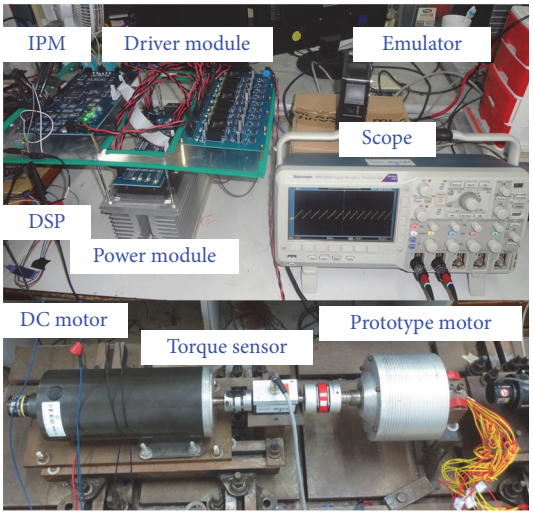

FIGURE 13: Prototype motor and experimental platform.

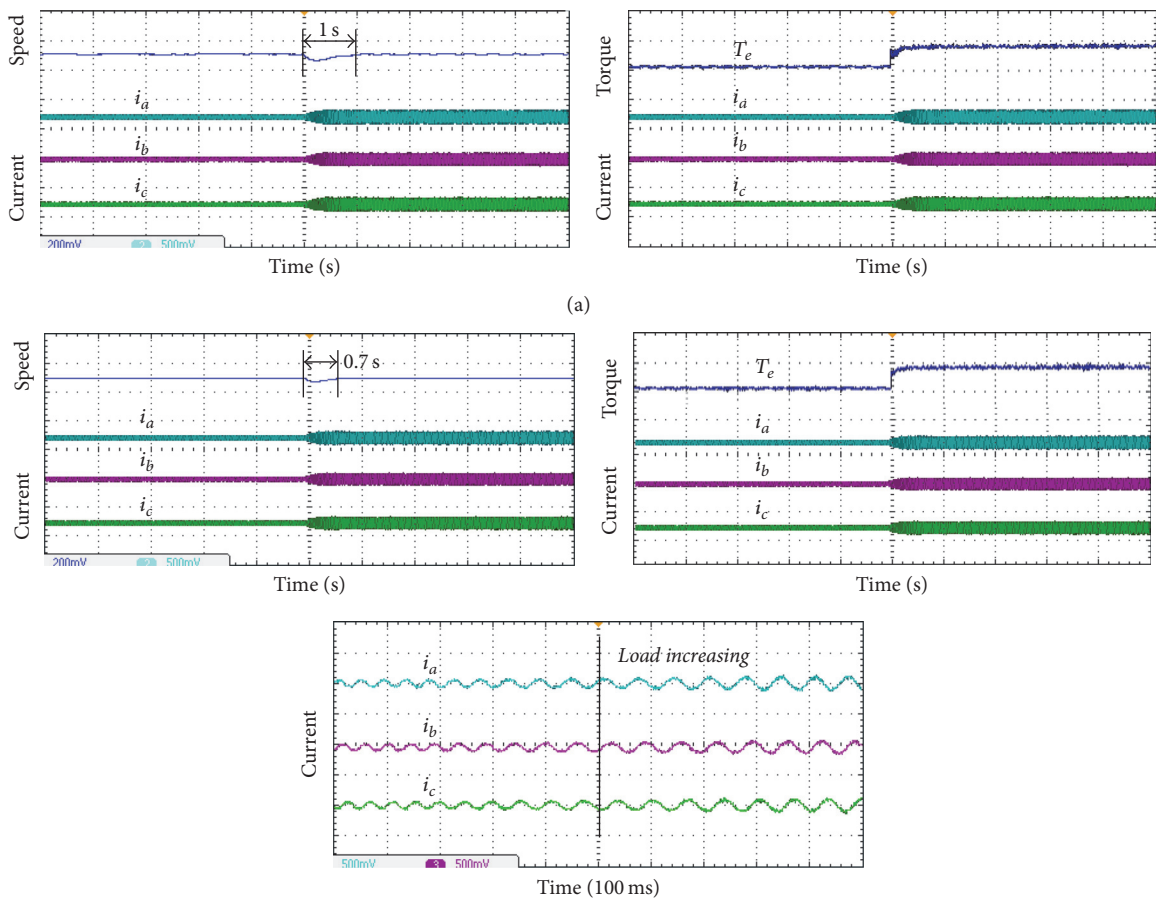

FIGURE 14: Response when the load suddenly increases (current (1 A/div), speed (200 r/min/div), torque (2 N·m/div), and time (1 s/div)). (a) The existing SMC control strategy. (b) The proposed SMC control strategy.

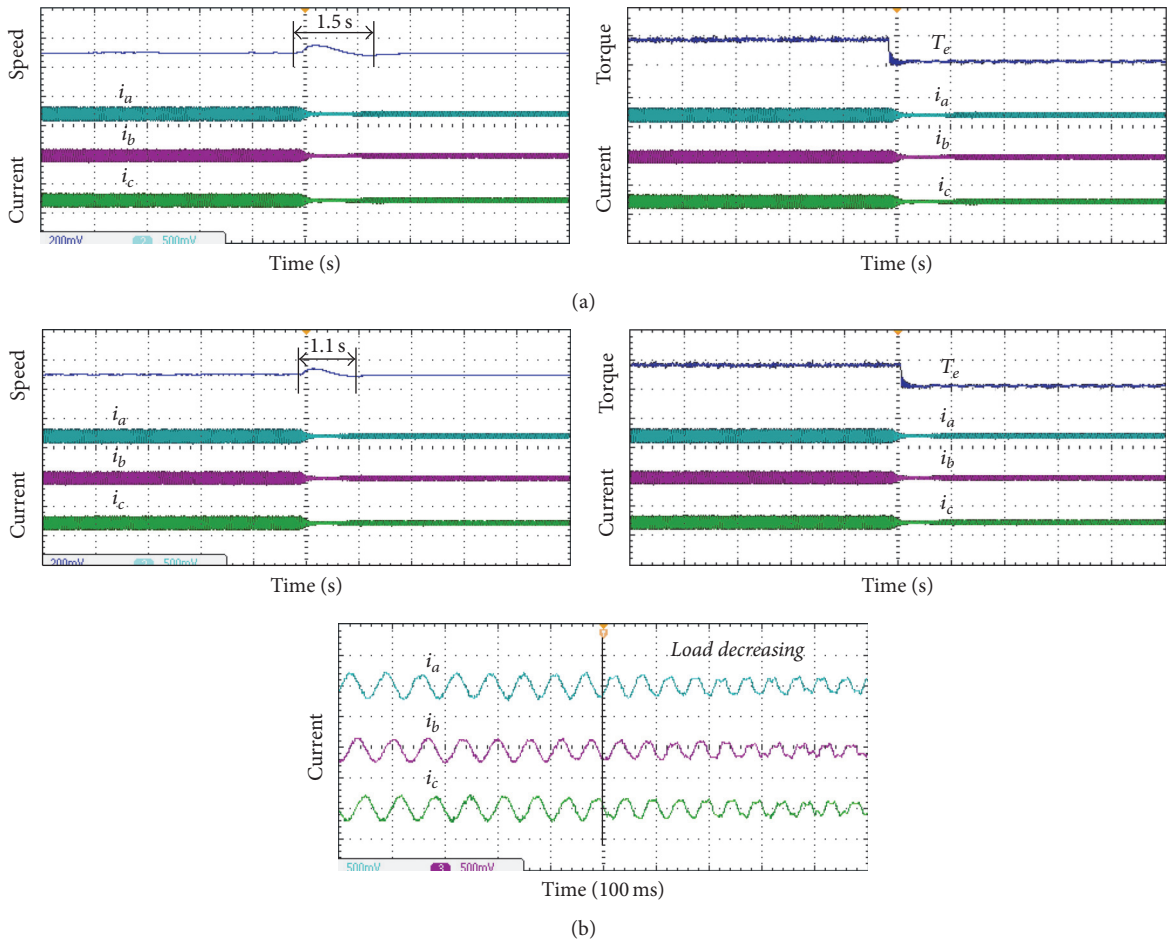

FIGURE 15: Response when the load suddenly decreases (current (1 A/div), speed (200 r/min/div), torque (2 N·m/div), and time (1 s/div)). (a) The existing SMC control strategy. (b) The proposed SMC control strategy.

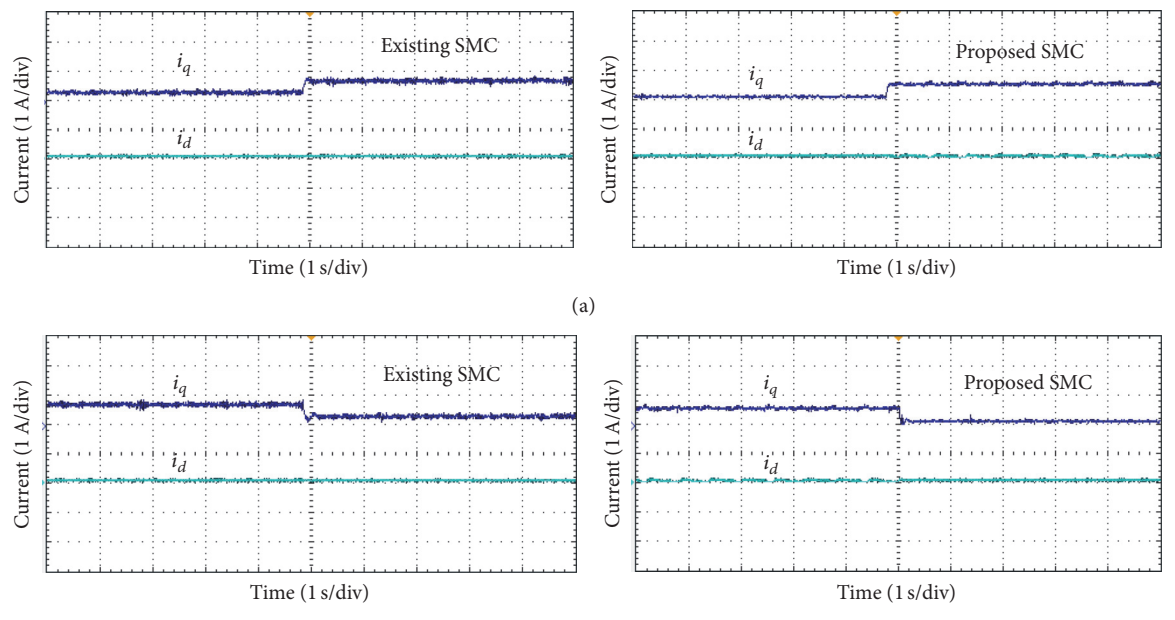

FIGURE 16: Measured waveforms of currents i_d and i_q. (a) With increasing load. (b) With decreasing load.

FT-FSPM motor, the next step of the research group will be to continue to study the medium-high speed performance of the motor.

Competing Interests

The authors declare that there is no conflict of interest regarding the publication of this paper.

Acknowledgments

This work was supported in part by the National Natural Science Foundation of China (Project no. 51422702).

References

[1] A. Mohammadpour and L. Parsa, "Global fault-tolerant control technique for multiphase permanent-magnet machines," *IEEE Transactions on Industry Applications*, vol. 51, no. 1, pp. 178–186, 2015.

[2] F. Aghili, "Energy-efficient and fault-tolerant control of multiphase nonsinusoidal PM synchronous machines," *IEEE/ASME Transactions on Mechatronics*, vol. 20, no. 6, pp. 2736–2751, 2015.

[3] N. K. Nguyen, F. Meinguet, E. Semail, and X. Kestelyn, "Fault-tolerant operation of an open-end winding five-phase PMSM drive with short-circuit inverter fault," *IEEE Transactions on Industry Electronics*, vol. 63, no. 1, pp. 595–605, 2016.

[4] J. Linares-Flores, C. García-Rodríguez, H. Sira-Ramírez, and O. D. Ramírez-Cárdenas, "Robust backstepping tracking controller for low-speed pmsm positioning system: design, analysis, and implementation," *IEEE Transactions on Industrial Informatics*, vol. 11, no. 5, pp. 1130–1141, 2015.

[5] F. F. M. El-Sousy, "Robust wavelet-neural-network sliding-mode control system for permanent magnet synchronous motor drive," *IET Electric Power Applications*, vol. 5, no. 1, pp. 113–132, 2011.

[6] V. Q. Leu, H. H. Choi, and J.-W. Jung, "Fuzzy sliding mode speed controller for PM synchronous motors with a load torque observer," *IEEE Transactions on Power Electronics*, vol. 27, no. 3, pp. 1530–1539, 2012.

[7] M. Caruso, V. Cecconi, A. O. Di Tommaso, and R. Rocha, "A rotor flux and speed observer for sensorless single-phase induction motor applications," *International Journal of Rotating Machinery*, vol. 2012, Article ID 276906, 13 pages, 2012.

[8] W. X. Zhao, M. Cheng, K. T. Chau, and C. C. Chan, "Control and operation of fault-tolerant flux-switching permanent-magnet motor drive with second harmonic current injection," *IET Electric Power Applications*, vol. 6, no. 9, pp. 707–715, 2012.

[9] M. Ali and P. Leila, "A unified fault-tolerant current control approach for five-phase PM motors with trapezoidal back EMF under different stator winding connections," *IEEE Transactions on Power Electronics*, vol. 28, no. 7, pp. 3517–3617, 2013.

[10] L. Dong, J. Jatskevich, Y. Huang, M. Chapariha, and J. Liu, "Fault diagnosis and signal reconstruction of hall sensors in brushless permanent magnet motor drives," *IEEE Transactions on Energy Conversion*, vol. 31, no. 1, pp. 118–131, 2015.

[11] C.-K. Lai and K.-K. Shyu, "A novel motor drive design for incremental motion system via sliding-mode control method," *IEEE Transactions on Industrial Electronics*, vol. 52, no. 2, pp. 499–507, 2005.

[12] X. Zhang, L. Sun, K. Zhao, and L. Sun, "Nonlinear speed control for PMSM system using sliding-mode control and disturbance compensation techniques," *IEEE Transactions on Power Electronics*, vol. 28, no. 3, pp. 1358–1365, 2013.

[13] J. Zhou and Y. Wang, "Adaptive backstepping speed controller design for a permanent magnet synchronous motor," *IEE Proceedings: Electric Power Applications*, vol. 149, no. 2, pp. 165–172, 2002.

[14] F. F. M. EIsousy, "Hybrid H^{∞}-based wavelet-neural-network tracking control for permanent-magnet synchronous motor servo drives," *IEEE Transaction on Industrial Electronics*, vol. 57, no. 9, pp. 3157–3166, 2010.

[15] S.-H. Chang, P.-Y. Chen, Y.-H. Ting, and S.-W. Hung, "Robust current control-based sliding mode control with simple uncertainties estimation in permanent magnet synchronous motor drive systems," *IET Electric Power Applications*, vol. 4, no. 6, pp. 441–450, 2010.

[16] S. Li and Z. Liu, "Adaptive speed control for permanent-magnet synchronous motors system with variations of load inertia," *IEEE Transactions on Industrial Electronics*, vol. 56, no. 8, pp. 3050–3059, 2009.

[17] N. T.-T. Vu, D.-Y. Yu, H. H. Choi, and J.-W. Jung, "T-S fuzzy-model-based sliding-mode control for surface-mounted permanent-magnet synchronous motors considering uncertainties," *IEEE Transactions on Industrial Electronics*, vol. 60, no. 10, pp. 4281–4291, 2013.

[18] Y. Feng, X. Yu, and F. Han, "High-order terminal sliding-mode observer for parameter estimation of a permanent-magnet synchronous motor," *IEEE Transactions on Industrial Electronics*, vol. 60, no. 10, pp. 4272–4280, 2013.

[19] H. Y. Kim, J. B. Son, and J. Y. Lee, "A high-speed sliding-mode observer for the sensorless speed control of a PMSM," *IEEE Transactions on Industrial Electronics*, vol. 58, no. 9, pp. 4069–4077, 2011.

[20] M. Marcin, "The adaptive backstepping control of permanent magnet synchronous motor supplied by current source inverter," *IEEE Transactions on Industrial Informatics*, vol. 9, no. 6, pp. 1047–1056, 2013.

[21] L. Yan, L. L. Shun, Z. S. Tuan, and L. Di, "Research of backstepping control for multiphase permanent magnet synchronous motor of two-motor series system," *International Journal of Grid and Distributed Computing*, vol. 8, no. 6, pp. 117–124, 2015.

[22] F. Mwasilu and J.-W. Jung, "Enhanced fault-tolerant control of interior PMSMs based on an adaptive EKF for EV traction applications," *IEEE Transactions on Power Electronics*, vol. 31, no. 8, pp. 5746–5758, 2016.

[23] B. Bossoufi, M. Karim, S. Ionita, and A. Lagrioui, "Low-speed sensorless control of pmsm motor drive using a nonlinear approach backstepping control: FPGA-based implementation," *Journal of Theoretical and Applied Information Technology*, vol. 36, no. 2, pp. 154–166, 2012.

[24] Z. Qiao, T. Shi, Y. Wang, Y. Yan, C. Xia, and X. He, "New sliding-mode observer for position sensorless control of permanent-magnet synchronous motor," *IEEE Transactions on Industrial Electronics*, vol. 60, no. 2, pp. 710–719, 2013.

[25] F.-J. Lin, I.-F. Sun, K.-J. Yang, and J.-K. Chang, "Recurrent fuzzy neural cerebellar model articulation network fault-tolerant control of six-phase permanent magnet synchronous motor position servo drive," *IEEE Transactions on Fuzzy Systems*, vol. 24, no. 1, pp. 153–167, 2016.